Dyes and Pigments 81 (2009) 203–210

Contents lists available at ScienceDirect

Dyes and Pigments

journal homepage: www.elsevier.com/locate/dyepig

Push–pull chromophores comprising benzothiazolium acceptor and thiophene auxiliary donor moieties: Synthesis, structure, linear and quadratic non-linear optical properties

Florence Quist [a], Christophe M.L. Vande Velde [a], Delphine Didier [a], Ayele Teshome [b], Inge Asselberghs [b], Koen Clays [b,**], Sergey Sergeyev [a,*]

[a] Laboratoire de Chimie des Polymères, Faculté des Sciences, Université Libre de Bruxelles (ULB), CP 206/01, Boulevard du Triomphe, 1050 Bruxelles, Belgium
[b] Department of Chemistry, University of Leuven, Celestijnenlaan 200D, 3001 Leuven, Belgium

ARTICLE INFO

Article history:
Received 1 August 2008
Received in revised form
15 September 2008
Accepted 10 October 2008
Available online 18 October 2008

Keywords:
Push–pull chromophores
Benzothiazolium
Thiophene
Non-linear optics
Second harmonic generation

ABSTRACT

Novel, push–pull chromophores combining a cationic benzothiazolium acceptor moiety and either one or two thiophene rings as a part of the conjugated π-system between the donor and the acceptor moieties have been synthesized and characterized. The chromophores displayed pronounced quadratic NLO activity with their first molecular hyper polarizabilities in agreement with their linear spectral properties.

1. Introduction

Interest in organic compounds with non-linear optical (NLO) properties is driven by the prospective of their applications in optical information technologies [1,2]. The most widely studied second-order (quadratic) NLO effects such as second harmonic generation (SHG) arise from high first molecular hyperpolarizabilities β. The most common design of molecules with large β values comprises strong electron-donors and acceptors connected by a π-conjugated system (donor–π–acceptor or "push–pull" chromophores). The vast majority of push–pull chromophores are neutral organic molecules, with all three key components (donor, acceptor and connecting π-system) varied very widely. At the same time, organic salts with an NLO-active cation (most often "stilbazolium" derivatives comprising the *N*-methylpyridinium cationic moiety as an acceptor) have also received considerable attention as they bring several interesting features: (1) cationic quaternary nitrogen is a very strong acceptor; (2) variation of counter ions is an easy way to tune the crystalline packing, (3) they are promising as amphiphilic materials for NLO-active Langmuir–Blodgett (LB) films [3–5]. Importantly, stilbazolium salts such as DAST (4′-dimethylamino-1-methyl-stilbazolium tosylate, [**1a**]OTs, Scheme 1) demonstrate very high second-order NLO activity in the bulk.

It was recently reported that the substitution of *N*-methylpyridinium with *N*-methylbenzothiazolium in stilbazolium vinylogues having up to four conjugated C=C bonds ([**1a**–**d**]PF_6, Scheme 1) has resulted in systematically larger first hyperpolarizability values for [**2a**–**d**]PF_6 [6]. This was correlated with systematic bathochromic shifts of the intramolecular charge transfer band in the electronic absorption spectra and was indicative of the stronger electron-withdrawing capacity of benzothiazolium compared to that of pyridinium. Furthermore, in a study of quadratic NLO in LB films, a benzothiazolium derivative was clearly superior to benzimidazolium and benzoxazolium analogues [7].

In the design of a conjugated π-system between donor and acceptor moieties in push–pull molecules, the incorporation of aromatic five-membered heterocycles has received much attention and often results in enhanced first molecular hyperpolarizability [8–18]. However, a delicate interplay of various factors must be taken into account; on the one hand, the aromaticity of the heterocycle is obviously important in providing efficient electron transfer between donor and acceptor moieties whilst, in contrast, it

* Corresponding author. Tel.: +32 2 6505392; fax: +32 2 6505410.
** Corresponding author.
E-mail addresses: Koen.Clays@fys.kuleuven.be (K. Clays), sserguee@ulb.ac.be (S. Sergeyev).

0143-7208/$ – see front matter © 2008 Elsevier Ltd. All rights reserved.
doi:10.1016/j.dyepig.2008.10.004

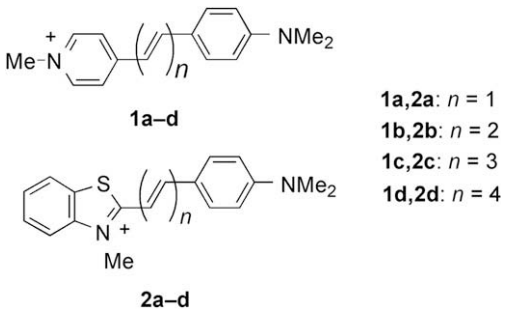

Scheme 1. Quadratic NLO properties of these two series of pyridinium ([**1a**–**d**]PF_6) and benzothiazolium ([**2a**–**d**]PF_6) cationic chromophores were systematically compared [6].

is clear that the electronic nature of the heteroaromatic ring will determine whether it acts as an "auxiliary donor" or an "auxiliary acceptor" [19]. Thiophene is a very good auxiliary donor insofar as it is electron-rich and, at the same time, is highly aromatic (compared with, for example, pyrrole or furane, which show more 1,3-diene character). Indeed, chromophores with thiophene as part of the bridging π-conjugated system display enhanced first molecular hyperpolarizabilities compared with pyrrole [11,20] or benzene [9,21–23] analogues.

With these considerations in mind, it was decided to explore the potential synthesis of push–pull chromophores for NLO-based applications, which combined the benzothiazolium cation as acceptor and one or more thiophene rings as auxiliary donors. This paper reports a proof-of-concept preliminary study comprising the synthesis, linear and quadratic non-linear properties of benzothiazolium iodides [**3a**–**c**]I.

2. Results and discussion

2.1. Synthesis

Synthesis of benzothiazolium chromophores [**3a**–**c**]I is depicted in Scheme 2. Starting bromoaldehydes **5a**, **c** are available commercially, while **5b** was prepared from 2-bromothiophene according to an earlier published procedure [24]. Bromoaldehydes **5a**–**c** were converted to the corresponding 4-(dimethylamino)-phenyl aldehydes **4a**–**c** by Suzuki coupling with commercially available 4-(dimethylamino)phenylboronic acid **6**. It should be noted that synthesis of aldehydes **4a** and **4c** by an alternative synthetic route (Negishi coupling between bromide **7** and either thiophen-2-yl or 2,2′-bithiophen-5-yl zinc(II) bromides followed by lithiation and reaction with Me_2NCHO) was reported earlier, but without experimental details or analytical data [25]. Synthesis of **4a** by Suzuki coupling between bromide **7** and thienylboronic acid **8** in fairly low yield (26%) was also reported recently (Scheme 2) [26]. However, a different and more logical disconnection of the aryl–aryl bond was used here by placing bromine on the thiophene ring, activated by an electron-withdrawing aldehyde group. This facilitates initial oxidative insertion of Pd(0) into the C–Br bond of **5a** compared to **7**, in which such insertion is strongly hampered by the pronounced electron-donating effect of Me_2N group. This difference in reactivity is reflected in considerably improved yield (67% of **4a** from **5a** vs. 26% of **4a** from **7**). Suzuki coupling of aldehydes **5b**, **c** with **6** also proceeded smoothly.

Finally, chromophores [**3a**–**c**]I were prepared via Knoevenagel condensation of 4-(dimethylamino)phenyl aldehydes **4a**–**c** with commercial methylbenzothiazolium iodide [**9**]I. A number of similar *N*-alkyl benzothiazolium derivatives featuring one or more conjugated C=C bonds were reported previously [6,27,28]. For the synthesis of [**3a**–**c**]I, we have adopted the published procedure for [**10**]I [29]. The latter was also synthesized by us from commercial 4-(dimethylamino)benzaldehyde and used as a benchmark molecule for the optical properties studies (see below). The yields of [**3a**–**c**]I given in Table 1 are those of analytically pure materials as used for the NLO experiments, crystallized twice from ethanol. Structures and purity of [**3a**–**c**]I were confirmed by IR, ^1H and ^{13}C NMR spectra, and by HRESIMS data. According to the ^1H NMR data, [**3a**–**c**]I crystallize as solvent-free molecules (contrary to [**10**]I that forms an 1:1 solvate with ethanol). As expected, CH=CH bonds in all chromophores [**3a**–**c**]I have a *trans* (*E*) configuration, as evidenced by the value of coupling constants $^3J_{H,H}$ for olefinic protons (see Table 1). Isomerization to the less thermodynamically stable

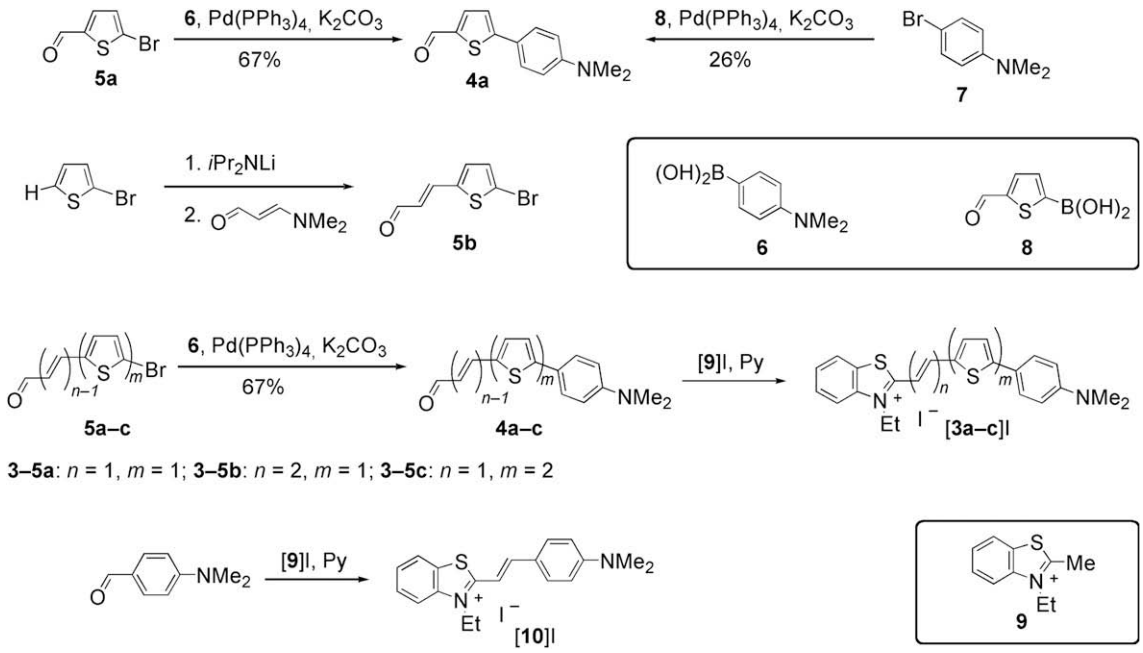

Scheme 2. Synthesis of cationic chromophores [**3a**–**c**]I and the key intermediates **4a**–**c**; Py = pyridine.

Table 1
Yields and selected properties of synthesized chromophores and intermediate aldehydes.

Derivative	Yield, %	$^3J_{CH=CH}$, Hz	λ_{max} (nm)/E (eV)[b]	ε_{max} (L mol^{-1} cm^{-1})[b]	λ_{end} (nm)/E (eV)[b]
4a	68	–	406/3.05	13300	520/2.38
4b	80	15.5	432/2.87	28600	540/2.30
4c	97	–	435/2.85	33300	560/2.21
[**3a**]I	49	15.0	636/1.95	53700	779/1.59
[**3b**]I	62	14.8, 14.3	655/1.89	54100	882/1.41
[**3c**]I	15	15.2	637/1.95	27000	897/1.38
[**10**]I	86[a]	15.3[a]	551/2.25	75400	638/1.94

[a] Data from our earlier published work [29].
[b] In CH_2Cl_2.

cis (*Z*)-isomers was not observed, even though no special protection against light was taken in the course of synthesis.

Chromophore [**3c**]I was obtained in very low isolated yield compared to its analogues [**3a**,**b**]I. There should not be, however, any fundamental reason for which the aldehyde **4c** would be less reactive in the Knoevenagel condensation compared to **4a**, **b**. The low isolated yield results from the difficulties with purification of [**3c**]I: due to its poor solubility it was only partially soluble in the solvents used for the crystallization, and this resulted in a considerable loss of material. Also UV–vis absorption spectra gave unexpectedly small apparent extinction coefficient, which may be explained by the tendency of [**3c**]I to form aggregates or colloidal particles together with a true solution.

2.2. Crystallography

Although the primary goal of this study was to investigate the second-order NLO response in solution, bulk NLO phenomena are of great importance. In the case of [**3a**]I, we have obtained single crystals suitable for an XRD study. The crystal structure of [**3a**]I is centrosymmetric: it crystallizes in space group *P*-1. In contrast to published analogues without thiophene ring [**2a**]PF_6, [**2a**]BPh_4, and [**2a**]OTs, which are nearly planar (the dihedral angles between the planes of dimethylamino-substituted benzene ring and the benzothiazolium ring do not exceed approx. 6°) [6], [**3a**]I has a twisted conformation (Fig. 1). While the benzothiazolium–CH=CH–thiophene part of the molecule is nearly coplanar (plane of CH=CH makes angles of 5.61(18)° and 1.78(19)° with the planes of the benzothiazolium and the thiophene rings), the angle between thiophene and benzene ring planes is 25.62(14)°. The overall twist of the molecule (the angle between the planes of dimethylamino-substituted benzene ring and the benzothiazolium ring) is equal to 38.44(11)°. This twist appears to originate from crystal packing forces.

Geometry optimization of [**3a**]$^+$, as well as of the other studied cations [**3b**,**c**]$^+$ and [**10**]$^+$, at the density functional theory (DFT) level yielded quasi-planar equilibrium conformations (Cartesian coordinates are available on request). A single point calculation for the crystal geometry of [**3a**]$^+$ yields an energy 34.1 kJ mol^{-1} higher than that of the planar equilibrium conformation, an energy difference which for a molecule of this size is certainly surmountable by packing forces. Furthermore, the Cambridge Structural Database search reveals a large spread in the observed conformations of thien-2-ylbenzene fragments. The maximum in the distribution of angles between thiophene and benzene ring is situated between 4 and 6° (e.g. ISEZIP/ISEZOF [30]), but it only tapers out slowly towards 40° (e.g. BIDLAC or RIFQED [31]). This confirms that the observed angle of ca. 25° in [**3a**]$^+$ is not unusual, and that the minimum in the potential for torsion around the thien-2-ylbenzene central bond is shallow.

The dimethylamino-substituted benzene ring displays some quinoid character pointing to partial charge separation in the ground state. Selected bond lengths are listed in Table 2. As could be expected, for the calculated planar equilibrium conformation, the quinoid character is slightly more pronounced than in the twisted solid-state structure.

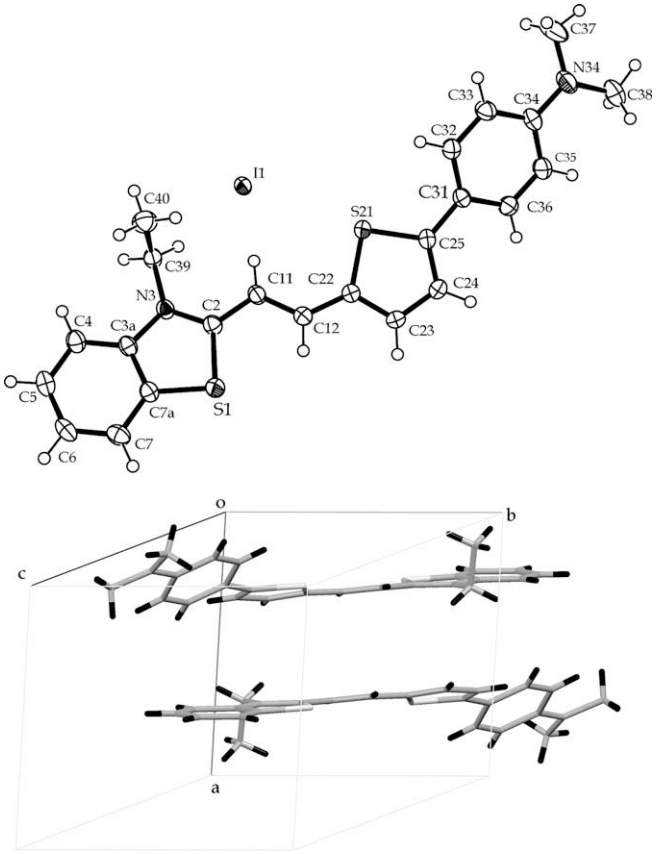

Fig. 1. ORTEP-style plot of [**3a**]I with displacement ellipsoids drawn at 50% probability level and the presentation of the packing of two cations of [**3a**]$^+$, dominated by the pair-wise π-stacking between thiophene and benzothiazolium moieties.

Finally, the packing of [**3a**]I appears to be dominated by both the pair-wise π-stacking between thiophene and benzothiazolium moieties (Fig. 1), and the creation of an apolar environment for the iodide anion. In previously published [**2a**]PF_6, [**2a**]BPh_4, and [**2a**]OTs without a thiophene ring [6], a similar motif of mutual π-stacking exists between the dimethylamino-substituted benzene ring and the benzothiazolium moiety. This may explain why these salts crystallize in centrosymmetric space groups and hence, will not display appreciable bulk NLO responses.

2.3. Linear spectral properties

The electronic absorption spectra of benzothiazolium chromophores [**3a**–**c**]I are dominated by the intense, broad low energy band due to intramolecular charge transfer (ICT).

As expected for these highly polar chromophores, their solubility is limited to the more polar solvents. For that reason, CH_2Cl_2,

Table 2
Selected bond distances in [**3a**]$^+$.

Bond[a]	Found from XRD, Å	Calculated by DFT, Å
C31–C32/C31–C36[b]	1.399(3)	1.4160
C33–C32/C35–C36[b]	1.380(3)	1.3779
C33–C34/C34–C35[b]	1.408(3)	1.4239
N34–C34	1.376(4)	1.3635
C25–C31	1.456(4)	1.4381

[a] For numbering of atoms, see Fig. 1.
[b] Average value for two bonds.

acetone and ethanol have been used in this study. Even in the fairly limited range of solvent polarity, a pronounced negative solvatochromism can be observed for [**3a–c**]I as well as for the reference chromophore [**10**]I (see Table 3 and Fig. 2). A blue shift of the charge transfer band is indeed observed upon going from least polar dichloromethane solvent ($\varepsilon = 9.1$) to more polar solvents (either acetone, $\varepsilon = 20.7$ or ethanol, $\varepsilon = 24.3$).

Solvatochromism is generally explained through differential solvation of the ground state and Franck–Condon excited state. Negative solvatochromism will result from better stabilization by polar solvents of the ground state in comparison to the excited state. The molecular orbitals involved in ICT in [**3a–c**]$^+$ and [**10**]$^+$ are depicted in Fig. 3. The HOMOs, as expected, are dominated by Me_2N group, and the LUMOs by the quaternary heterocyclic moiety. On excitation, electron density is transferred from the donor end of the molecule to the positively charged quaternary heterocyclic moiety, providing charge compensation, and thus indeed resulting in an excited state that is less polar than the ground state, and hence less stabilized by polar solvents. Therefore, negative solvatochromism should be expected. This situation is opposite to push–pull molecules with neutral donor and acceptor functions such as 4-dimethylamino-4′-nitrostilbene (DANS), where due to the absence of a positive charge, ICT produces more polar excited state with formal positive charge on the donor and a negative one on the acceptor. Indeed, DANS and similar molecules are well known to exhibit pronounced positive solvatochromism [32].

The experimentally observed negative solvatochromism of [**3a–c**]$^+$ constitutes convincing evidence for a ground state that is more polar than the charge-transfer excited state, and is in perfect agreement with previous observations on the series of chromophores [**1a–d**]PF_6 and [**2a–d**]PF_6 [6] and many other benzothiazolium chromophores [27]. On the other hand, systematic red shifts going from acetone to more polar ethanol suggest importance of other solvent properties, such as hydrogen bond donor or acceptor capacity. Detailed study of solvatochromism of [**3a–c**]I may provide interesting information. This was not, however, the purpose of the present work. It is worth mentioning that chromophores [**3a–c**]I featuring a thiophene auxiliary donor show more pronounced solvatochromism compared to the benchmark chromophore [**10**]I (cf. $\Delta E = 0.24$–0.27 eV for [**3a–c**]I vs. 0.12 eV for [**10**]I), and might therefore be interesting as solvent polarity probes.

Within a constant solvent polarity, an extension of the conjugation path between the donor and acceptor moiety often shifts the wavelength of the absorption band to the red, and this systematic shift is typically accompanied by an increase in the first molecular polarizability [33–35]. In our case, incorporation of a thiophene auxiliary donor into the π-system indeed results in a clear bathochromic shift ([**3a**]I vs. [**10**]I, see Table 3). However, addition of a second thienyl unit in the conjugated system of a chromophore barely has an effect on the absorption maximum ([**3c**]I vs [**3a**]I). Adding a second ethenyl group has a relatively small effect, in particular in highly polar solvents ([**3b**]I vs [**3a**]I). This appears unexpected at first glance, because, for example, in case of aldehydes **4a–c** addition of a thiophene ring or a C=C bond caused pronounced red shifts of the absorption maximum (see Table 1).

Table 3
Absorption maxima of [**3a–c**]I and [**10**]I in different solvents.

Chromophore	λ_{max} (nm)/E (eV), in ethanol	λ_{max} (nm)/E (eV), in acetone	λ_{max} (nm)/E (eV), in CH_2Cl_2	ΔE (eV)[a]
[**10**]I	528/2.35	522/2.37	551/2.25	0.12
[**3a**]I	582/2.13	566/2.19	636/1.95	0.24
[**3b**]I	591/2.10	574/2.16	655/1.89	0.27
[**3c**]I	579/2.14	568/2.18	637/1.95	0.23

[a] Difference in energy of absorption going from acetone to CH_2Cl_2.

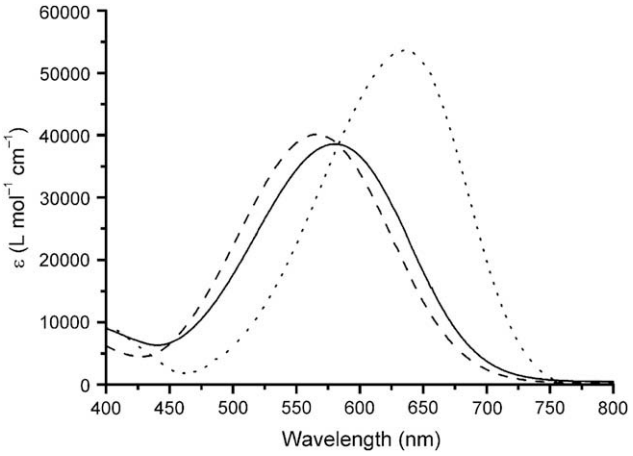

Fig. 2. Electronic absorption spectra of [**3a**]I in ethanol (solid line), acetone (dashed line) and CH_2Cl_2 (dotted line).

The observed relationships between structure and absorption maxima of studied chromophores should be interpreted with caution. It is well established that in the series of conjugated molecules with repeating π-systems (often referred to as "conjugated oligomers"), the energy of the electron transition monotonously decreases with increasing number of repeating π-systems until the latter achieves an effective conjugation length (ECL), beyond which further extension of π-system has no measurable effect. Accordingly, the maxima of the long-wave absorptions should undergo monotonous bathochromic shift with increasing number of repeating units (n), and reach saturation upon approaching ECL [36]. However, behavior of conjugated oligomers bearing strong donors and acceptors at the termini of π-system is, in general, more complex. This is due to the fact that the energy of the electron transition should now be considered as a sum of two terms: E_s, which takes into account the conjugation of purely donor or purely acceptor substituted π-system, and $-\Delta E_{DA}$ that describes efficiency of interaction between donor and acceptor. With an increasing number of repeating units (n), E_s has a monotonously declining and $-\Delta E_{DA}$ a monotonously rising function. The summation of the two functions may, however, give different

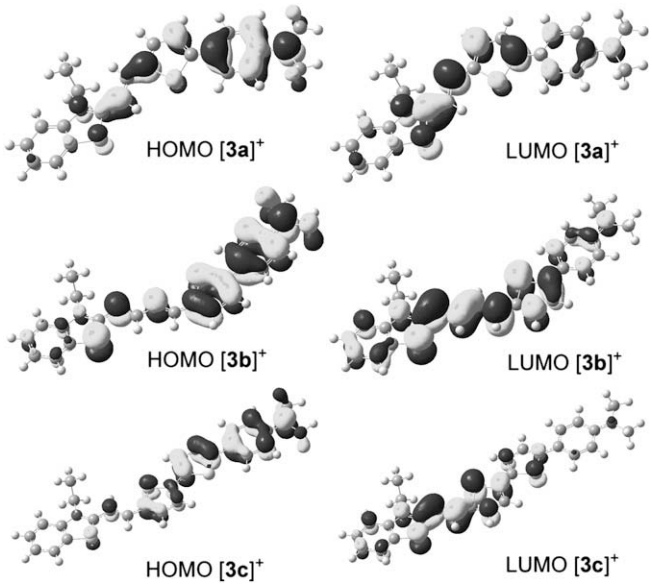

Fig. 3. Shape of the HOMO (left) and LUMO (right) of [**3a–c**]$^+$.

Table 4
End-absorption wavelengths and energies of [**3a–c**]I and [**10**]I in different solvents.

Chromophore	λ_{end} (nm)/E (eV), in ethanol	λ_{end} (nm)/E (eV), in acetone	λ_{end} (nm)/E (eV), in CH_2Cl_2	Calculated HOMO/LUMO gap (eV)
[**10**]I	640 (1.94)	608 (2.04)	638 (1.94)	2.65
[**3a**]I	750 (1.65)	743 (1.67)	779 (1.59)	2.07
[**3b**]I	826 (1.50)	813 (1.53)	882 (1.41)	1.87
[**3c**]I	780 (1.59)	820 (1.51)	897 (1.38)	1.64

results. Indeed, very often an "expected" overall monotonous increase of E_s–ΔE_{DA} is observed. This is for example the case for the above-mentioned vinylogous benzothiazolium salts [**2a–d**]PF_6, which clearly show bathochromic shifts with a trend to saturation upon increase of the conjugation length. Thus, addition of one CH=CH unit caused a red shift of 0.17–0.24 eV (in various solvents) between **2a** and **2b**, but only 0.02–0.04 eV between **2c** and **2d** [6].

On the other hand, E_s–ΔE_{DA} has been shown to display different behaviors as a function of n. In some instances, monotonous hypsochromic shift was observed [37–40]. As a border case between monotonous hypso- and bathochromic shifts, E_s–ΔE_{DA} can be nearly independent of the π-system length [22]. E_s–ΔE_{DA} can also go through a minimum, leading to a maximum of λ_{max} at certain n [38,41], or go through a maximum, which would correspond to a minimum of λ_{max} at certain n. The latter theoretically possible case still remains to be reported (see the comprehensive review by Meier [22] for in-depth discussion).

Taking all of this into account, it is unwise to make premature conclusions about relationships between structure of the chromophores [**3a–c**]I, [**10**]I and their linear optical properties. Although we generally increase the length of the conjugated π-system from [**10**]I to [**3a**]I and then to [**3b**,**c**]I, these molecules do not form a series of conjugated oligomers. The detailed study of this issue is undoubtedly interesting and in the future, we plan to perform more systematic variation of the conjugated system while keeping the same donor and acceptor moieties, as well as vary the cationic acceptor moieties within these series. Taking into account poor solubility that was encountered already with a relatively modest size of the π-system (in the case of [**3c**]I), installation of "solubilizing" longer alkyl substituents on the amino group of the donor and/or on the quaternary nitrogen atom of the cationic acceptor appears unavoidable.

The values of end-absorption wavelength λ_{end} are useful to consider since they provide an experimental estimation for the HOMO–LUMO gaps of conjugated molecules and show good correlation with the length of the conjugated π-system of push–pull chromophores [42]. Indeed, in our case the expansion of the π-conjugated system from [**10**]I to [**3a**]I and then to [**3b**,**c**]I resulted in systematic increase of the end-absorption wavelength in all studied solvents. Theoretically calculated HOMO–LUMO gaps for quasi-planar DFT-optimized geometries of $[\mathbf{3a–c}]^+$ and $[\mathbf{10}]^+$ faithfully reproduce the trend seen in the experimental values as derived from the end-absorption wavelengths, but the numerical values are systematically overestimated by approx. 25% (see Table 4).

2.4. Quadratic NLO properties

To test our hypothesis that incorporation of a thiophene ring in the π-conjugated system of cationic push–pull chromophores will increase their second-order non-linear optical response, we performed hyper-Rayleigh scattering (HRS) experiments in ethanol at 800 nm for [**3a–c**]I as well as for the benchmark chromophore [**10**]I, which lacks the thiophene auxiliary donor, in DMF. Due to solubility problems of [**10**]I in the concentration range for HRS measurements, this compound is measured in DMF. Since only a small shift (3 nm) in λ_{max} is observed between the ethanol and the DMF solvent we still will refer to it as the benchmark compound. These measurements have been analyzed towards a single major hyperpolarizability tensor component β_{zzz} along the unique molecular z-axis.

The dynamic values $\beta_{zzz,800\ nm}$ do show a significant variation between the four chromophores studied (Table 5). This was expected, based on the variation of the charge-transfer transition energy. To extract this inherent dependence, known as the resonance enhancement effect, the static $\beta_{zzz,0}$ value can be derived based on the simple two-level model. While this model might be too simplified (no damping included) and the resonance wavelength is too close to the measurement wavelength to be valid in absolute terms, this is true for all four compounds. The relative error that would be introduced is therefore conjectured to be approximately identical for all four chromophores studied. The introduction of a thiophene unit in [**3a**]I leads not only to a large red-shift in λ_{max} but to the doubling of the hyperpolarizability β_{zzz}. The insert of an additional C=C from [**3a**]I to [**3b**]I results in an strong increase on the hyperpolarizability β_{zzz}. While the addition of another thiophene unit to [**3a**]I, leading to [**3c**]I, results in a small decrease in the hyperpolarizability as compared to [**3a**]I, which is in agreement with the expectations from the linear spectral data obtained.

3. Conclusions

We have synthesized novel push–pull chromophores combining a cationic benzothiazolium acceptor moiety with one or two thiophene rings as part of the π-system between the donor and the acceptor moieties. Adding an auxiliary thiophene donor ring produced, as expected, a remarkable bathochromic shift of the intramolecular charge transfer band in the absorption spectra. However, further addition of either one more thiophene ring to the conjugation system, or one more C=C bond, caused only minor changes in the absorption spectra. As discussed in the text, it is difficult to draw conclusions concerning structure–property relationships at this point. In the future, we plan a more systematic study of this issue on further chromophores combining thienyl and ethenyl moieties in the bridging π-system between the di-alkylamino donor and quaternary cation acceptor groups.

All the synthesized chromophores have shown pronounced quadratic NLO activity. The insert of a thiophene unit induces a doubling of the NLO response as compared to that of a reference system featuring an identical acceptor but lacking the auxiliary thiophene donor. However, further addition of a thiophene unit

Table 5
Non-linear optical measurement data of [**3a–c**]I and [**10**]I in ethanol.

Chromophore	λ_{max} (nm)	$<\beta_{zzz,800\ nm}>$ (10^{-30} esu)	$\beta_{zzz,800\ nm,0\ MHz}$ (10^{-30} esu)	Slope (10^{-30} esu MHz^{-1})	$\beta_{zzz,0}$ (10^{-30} esu)
[**10**]I	525	290 ± 10	270 ± 2	0.09 ± 0.01	120 ± 5
[**3a**]I	582	580 ± 20	590 ± 30	−0.05 ± 0.20	300 ± 10
[**3b**]I	591	1240 ± 50	1340 ± 120	−0.66 ± 0.79	660 ± 25
[**3c**]I	579	430 ± 30	440 ± 15	−0.12 ± 0.10	220 ± 15

leads to a leveling of the hyperpolarizabitlity while the insert of the C=C bond leads to an increase in NLO activity.

4. Experimental section

4.1. General

All chemicals were purchased from Aldrich or Acros and used without further purification unless stated otherwise. Aldehyde **5b** was prepared according to the published procedure [24]. Column chromatography: SiO_2 Kieselgel 60 (Macherey–Nagel, particle size 0.04–0.063 mm). TLC: precoated SiO_2 plates Kieselgel $60F_{254}$ (Merck). ^1H NMR (300 MHz) and ^{13}C NMR (75 MHz) spectra were recorded in $CDCl_3$ or $(CD_3)_2SO$ on a Bruker Avance 300 spectrometer; chemical shifts (δ) are given in ppm relative to Me_4Si (internal standard); coupling constants (J) are given in Hz. Electron impact mass spectra (EIMS) were recorded on a Waters AutoSpec 6F instrument and electrospray ionization mass spectra (ESIMS) on a Waters QToF 2 instrument; m/z with the lowest isotopic mass are reported. UV/vis spectra (λ_{max} [nm], (ϵ_{max} [$m^{-1}\,cm^{-1}$])) were recorded on Agilent 8453 spectrophotometer, in 1 cm quartz cell at ambient temperature. In order to determine the end-absorption wavelength of broad ICT bands as precise as possible, the first derivative of the absorption vs. wavelength curve was built and the value at which the first derivative approaches zero was determined. Fluorescence experiments were realized on an Aminco–Bowman series 2 spectrophotometer.

4.1.1. 5-(4-Dimethylaminophenyl)thiophenyl-2-carbaldehyde (**4a**)

To the mixture of aldehyde **5a** (191 mg, 1.0 mmol), $Pd(PPh_3)_4$ (116 mg, 0.1 mmol), and toluene (20.0 mL), a suspension of boronic acid **6** (198 mg, 1.20 mmol) in ethanol (7 mL) and a solution of K_2CO_3 (1.38 g, 10 mmol) in water (2.0 mL) were added. The mixture was heated to reflux in an argon atmosphere for 3 h. After cooling to room temperature, the mixture was filtered through Celite and the organic phase was washed with water (3 × 10 mL). The organic layer was then dried over $MgSO_4$ and concentrated under vacuum. Column chromatography (CH_2Cl_2) of the residue afforded **5a** as an orange powder (0.157 g). Yield 68%; mp 203–205 °C (Ref. [26] 189–190 °C); other analytical data were identical to those published earlier [26].

4.1.2. (E)-3-[5-(4-Dimethylaminophenyl)thiophen-2-yl]-propenal (**4b**)

Prepared similarly to **4a** from **5b** (217 mg, 1.0 mmol). Purification by column chromatography (CH_2Cl_2) afforded **4b** (0.205 g) as an orange powder. Yield 80%; mp 213–215 °C;. ^1H NMR ($CDCl_3$, 300 MHz, 25 °C): $\delta = 3.01$ (s, 6H), 6.43 (dd, $^3J_{H,H} = 15.5$ Hz $^3J_{H,H} = 7.8$ Hz, 1H), 6.71 (d, $^3J_{H,H} = 9.0$ Hz, 2H), 7.15 (d, $^3J_{H,H} = 3.9$ Hz, 1H), 7.28 (d, $^3J_{H,H} = 3.9$ Hz, 1H), 7.52 (d, $^3J_{H,H} = 9.0$ Hz, 2H), 7.54 (d, $^3J_{H,H} = 15.5$ Hz, 1H), 9.59 (d, $^3J_{H,H} = 7.8$ Hz, 1H). ^{13}C NMR ($CDCl_3$, 75 MHz, 25 °C): $\delta = 40.3, 112.2, 121.3, 121.9, 125.6, 127.1, 134.2, 136.1, 144.9, 150.8, 151.3, 192.8$; HRESIMS: m/z calcd for $C_{15}H_{16}NOS$ ($[M+H]^+$): 258.0953; found 258.0955; UV–visible (CH_2Cl_2) $\lambda_{max} = 432$ nm, $\varepsilon_{432} = 28600\ L\,mol^{-1}\,cm^{-1}$; IR(KBr) ($\nu_{max}/cm^{-1}$): 2845, 1657 (C=O), 1593, 1435, 1365, 1271, 1198, 1159, 1159, 1119, 1053, 810.

4.1.3. 5′-(4-Dimethylaminophenyl)-[2,2′]-bithiophenyl-5-carbaldehyde (**4c**)

Prepared similarly to **4a** from **5c** (273 mg, 1.0 mmol). Purification by column chromatography (CH_2Cl_2) afforded **4c** (0.303 g) as an orange powder. Yield 97%; mp 235–236 °C;. ^1H NMR ($CDCl_3$, 300 MHz, 25 °C): $\delta = 3.00$ (s, 6H), 6.72 (d, $^3J_{H,H} = 9.0$ Hz, 2H), 7.11 (d, $^3J_{H,H} = 3.9$ Hz, 1H), 7.21 (d, $^3J_{H,H} = 3.9$ Hz, 1H), 7.30 (d, $^3J_{H,H} = 3.9$ Hz, 1H), 7.49 (d, $^3J_{H,H} = 9.0$ Hz, 2H), 7.66 (d, $^3J_{H,H} = 3.9$ Hz, 1H), 9.84 (s, 1H); NMR ^{13}C ($CDCl_3$, 75 MHz, 25 °C): $\delta = 40.4, 112.4, 121.6, 121.8, 123.3, 126.9, 127.3, 132.7, 137.6, 140.8, 147.6, 148.0, 150.4, 182.4$; HREIMS: m/z calcd for $C_{17}H_{15}NOS_2$ ($[M]^+$) 313.0595; found 313.0592; UV–visible (CH_2Cl_2) $\lambda_{max} = 435$ nm, $\varepsilon_{435} = 33300\ L\,mol^{-1}\,cm^{-1}$; IR (KBr) ($\nu_{max}/cm^{-1}$): 2850, 2930, 1653 (C=O), 1606, 1547, 1454, 1456, 1367, 1230, 1049, 794, 752, 667.

4.1.4. (E)-2-[2-[5-(4-Dimethylaminophenyl)thiophen-2-yl]ethenyl]-3-ethyl benzothiazol-3-ium iodide ([**3a**]I)

A mixture of **4a** (230 mg, 0.994 mmol), 3-ethyl-2-methyl-benzothiazolium iodide [**9**]I (270 mg, 0.885 mmol) and pyridine (0.120 mL) in ethanol (11.5 mL) was heated to reflux for 18 h. The reaction mixture was then cooled to room temperature, the precipitated solid was filtered, and then crystallized twice from ethanol to afford [**3a**]I (225 mg) as a green crystalline solid. Yield 49%; mp 250–254 °C;. ^1H NMR (DMSO-d_6, 300 MHz, 25 °C): $\delta = 1.45$ (t, $^3J_{H,H} = 7.2$ Hz, 3H), 3.00 (s, 6H), 4.87 (q, $^3J_{H,H} = 7.2$ Hz, 2H), 6.79 (d, $^3J_{H,H} = 8.9$ Hz, 2H), 7.49 (d, $^3J_{H,H} = 15.0$ Hz, 1H), 7.58 (d, $^3J_{H,H} = 4.0$ Hz, 1H), 7.64 (d, $^3J_{H,H} = 8.9$ Hz, 2H), 7.74 (dd, $^3J_{H,H} = 7.5$ Hz, $^3J_{H,H} = 8.0$ Hz, 1H), 7.83 (dd, $J = 8.0$ Hz, $^3J_{H,H} = 8.5$ Hz, 1H), 7.93 (d, $^3J_{H,H} = 4.0$ Hz, 1H), 8.21 (d, $^3J_{H,H} = 8.5$ Hz, 1H), 8.38 (d, $^3J_{H,H} = 7.5$ Hz, 1H), 8.40 (d, $^3J_{H,H} = 15.0$ Hz, 1H); ^{13}C NMR (DMSO-d_6, 75 MHz, 25 °C): $\delta = 13.9, 39.6, 43.8, 108.4, 112.1, 116.0, 119.8, 123.1, 124.1, 127.1, 127.6, 127.8, 129.2, 135.7, 138.6, 140.8, 141.7, 151.0, 154.2, 170.2$; HRESIMS: m/z calcd for $[C_{23}H_{23}N_2S_2]^+$ ([**3a**]$^+$): 391.1303; found: 391.1300; IR (KBr) (ν_{max}/cm^{-1}): 1578, 1512, 1419, 1369, 1317, 1269, 1213, 1209, 1068, 951, 810, 766.

4.1.5. (E,E)-2-[4-[5-(4-Dimethylaminophenyl)-thiophen-2-yl]buta-1,3-dienyl]-3-ethyl benzothiazol-3-ium iodide ([**3b**]I)

Prepared similarly to [**3a**]I from **4b** (231 mg, 0.898 mmol), [**9**]I (169 mg, 0.553 mmol) and pyridine (60 μL) in ethanol (6.0 mL). The crude product was crystallized twice from ethanol to afford [**3b**]I (188 mg) as a green powder. Yield 62%; mp 260–263 °C;. ^1H NMR (DMSO-d_6, 300 MHz, 25 °C): $\delta = 1.45$ (t, $^3J_{H,H} = 7.2$ Hz, 3H), 2.98 (s, 6H), 4.76 (q, $^3J_{H,H} = 7.2$ Hz, 2H), 6.76 (d, $^3J_{H,H} = 9.0$ Hz, 2H), 7.05 (dd, $^3J_{H,H} = 14.8$ Hz, $^3J_{H,H} = 10.7$ Hz, 1H), 7.43 (d, $^3J_{H,H} = 3.8$ Hz, 1H), 7.46 (d, $^3J_{H,H} = 3.8$ Hz, 1H), 7.55 (d, $^3J_{H,H} = 14.3$ Hz, 1H), 7.55 (d, $^3J_{H,H} = 9.0$ Hz, 2H), 7.66 (d, $^3J_{H,H} = 14.8$ Hz), 7.74 (td, $^3J_{H,H} = 7.7$ Hz, $^3J_{H,H} = 0.7$ Hz, 1H), 7.83 (td, $^3J_{H,H} = 7.7$ Hz, $^3J_{H,H} = 1.0$ Hz, 1H), 8.02 (dd, $^3J_{H,H} = 14.3$ Hz, $^3J_{H,H} = 10.7$ Hz, 1H), 8.23 (d, $^3J_{H,H} = 7.7$ Hz, 1H), 8.38 (dd, $^3J_{H,H} = 7.7$ Hz, $^3J_{H,H} = 1.0$ Hz, 1H); ^{13}C NMR (DMSO-d_6, 75 MHz, 25 °C): $\delta = 13.8, 44.0, 112.2, 114.0, 116.1, 120.3, 122.7, 124.2, 125.1, 126.7, 127.88, 127.91, 129.3, 134.5, 137.5, 138.5, 140.7, 149.58, 149.61, 150.5, 170.0$ (signal of Me_2N is overlapped with the signal from residual non-deuterated solvent); HRESIMS: m/z calcd for $[C_{25}H_{25}N_2S_2]^+$ ([**3b**]$^+$) 417.1459; found 417.1462; IR (KBr) (ν_{max}/cm^{-1}): 3005, 1576, 1479, 1423 (s), 1363, 1356, 1282, 1155, 1061, 984, 762.

4.1.6. (E)-2-[2-[5′-(4-Dimethylaminophenyl)[2,2′]bithiophenyl-5-yl]ethenyl]-3-ethyl benzothiazol-3-ium iodide ([**3c**]I)

Prepared similarly to [**3a**]I from **4c** (238 mg, 0.759 mmol), [**9**]I (255 mg, 0.836 mmol) and pyridine (0.090 mL) in ethanol (14.0 mL). The crude product was first washed several times with hot toluene and then crystallized twice from ethanol to afford [**3c**]I (68 mg) as a green powder. Yield 15%; mp 240–243 °C;. ^1H NMR (DMSO-d_6, 300 MHz, 25 °C): $\delta = 1.46$ (t, $^3J_{H,H} = 7.0$ Hz, 3H), 2.97 (s, 6H, 1H), 4.90 (q, $^3J_{H,H} = 7.0$ Hz, 2H), 6.76 (d, $^3J_{H,H} = 9.1$ Hz, 2H), 7.40 (d, $^3J_{H,H} = 3.9$ Hz, 1H), 7.44–7.57 (m, 2H), 7.61 (d, $^3J_{H,H} = 15.2$ Hz, 1H), 7.76 (dd, $^3J_{H,H} = 7.1$ Hz, $^3J_{H,H} = 7.9$ Hz, 1H), 7.85 (dd, $^3J_{H,H} = 7.1$ Hz, $^3J_{H,H} = 8.3$ Hz, 1H), 7.93 (d, $^3J_{H,H} = 4.2$ Hz, 1H), 8.24 (d, $^3J_{H,H} = 8.2$ Hz, 1H), 8.40 (d, $^3J_{H,H} = 7.9$ Hz, 1H), 8.44 (d, $^3J_{H,H} = 15.2$ Hz). HRESIMS: m/z calcd for $[C_{27}H_{25}N_2S_3]^+$ ([**3c**]$^+$) 473.1180; found 473.1176; IR (KBr) (ν_{max}/cm^{-1}): 3479, 3014, 1606, 1576, 1417, 1375, 1267, 1277, 1223, 1053, 958, 797.

4.2. Theoretical calculations

All calculations were performed in Gaussian 03 [43] with the DFT method at the B3LYP level with a 6-31G* basis set. All chromophores were geometry-optimized, and frequency calculations performed on the final geometries, in order to ascertain that they were indeed minima. No imaginary frequencies were found. For the single point calculation of the crystal conformation of [**3a**]$^+$, the bond lengths to hydrogen atoms were set from their XRD lengths to the values found in the optimized geometry.

4.3. XRD crystal structure analysis of [*3a*]I

Crystals were grown by slow evaporation of a drop of DMSO solution on a glass microscope slide. Crystal data at 140(2) K: $C_{23}H_{23}IN_2S_2$, $M_r = 518.45$, crystal size $0.19 \times 0.19 \times 0.05$ mm, triclinic, space group *P*-1, $Z = 2$, $a = 9.2117(12)$ Å, $b = 10.0881(13)$ Å, $c = 12.2193(16)$ Å, $\alpha = 97.161(2)^\circ$, $\beta = 93.354(2)^\circ$, $\gamma = 100.723(2)^\circ$, $V = 1103.1(2)$ Å^3, $\rho_{calcd} = 1.561$ g cm^{-3}. Data were collected on a Bruker AXS SMART APEX CCD diffractometer system with sealed tube Mo source, $\lambda = 0.71073$ Å. Data were collected, integrated and corrected for absorption with the Bruker software package. The structure was solved by direct methods (SHELXS-97) and refined by full-matrix least squares on all F_o^2 using SHELXL-97 [44]. Hydrogen atoms could clearly be seen in the difference maps. The aromatic hydrogen atoms were refined as riding on their parent atom, for methylene groups also the distance was allowed to refine, and for methyl groups both distances and torsion angle were allowed to refine. Data collection: $1.69 < \theta < 30.70^\circ$, reflections collected: 13052, independent reflections: 6656 [$R(\text{int}) = 0.0220$], parameters: 260, goodness-of-fit on F^2: 1.090. Final $R(F) = 0.0358$, w$R(F^2) = 0.0723$ for $I > 2\sigma(I)$, $R(F) = 0.0473$, w$R(F^2) = 0.0785$ for all data.

Crystallographic data (excluding structure factors) for the structure in this paper have been deposited with the Cambridge Crystallographic Data Centre as supplementary publication no. CCDC 691314. Copies of the data can be obtained, free of charge, on application to CCDC, 12 Union Road, Cambridge CB2 1EZ, UK, (fax: +44 (0)1223 336033 or e-mail: deposit@ccdc.cam.ac.uk).

4.4. NLO measurements

Since the benchmark chromophore [**10**]I is ionic and known to be fluorescent [27], the NLO experiments were performed on a femtosecond hyper-Rayleigh scattering set-up with the capability to discriminate between immediate non-linear scattering and time-delayed fluorescence, if present [45,46]. The measurements were performed in ethanol or DMF, crystal violet in methanol (octupolar β_{xxx} value of 338×10^{-30} esu) was used as a reference. The differences in symmetry (octupolar vs. assumed dipolar) and solvent were taken into account by proper weighing of the tensor component contribution to the HRS signal and by proper solvent correction factor, respectively. These measurements produce an apparent first hyperpolarizability, $\beta_{zzz,800\ nm}$, dependent on the amplitude modulation frequency. A non-zero slope is indicative of the presence of fluorescence. From the small values of this slope, relative to the larger estimated uncertainty on this value, it is concluded that there is no frequency dependence, and, hence, no fluorescence contributing to the hyper-Rayleigh scattering signal. To support this conclusion, the fluorescence behavior of the newly synthesized chromophores [**3a**–**c**]I was also studied. Surprisingly, [**3a**,**c**]I exhibited only very little or no fluorescence, contrary to the benzothiazolium chromophore [**10**]I that is highly fluorescent in various solvents [27].

For the benchmark chromophore [**10**]I, measurements were performed up to 480 MHz amplitude modulation frequency while for the new compounds, the measurements up to 400 MHz also did not indicate fluorescence. From the observed zero slope, there is very good agreement between the intercept $\beta_{zzz,800\ nm,0\ MHz}$ of the apparent hyperpolarizability value ($\beta_{zzz,800\ nm}$ at 0 MHz modulation frequency) and the average value $<\beta_{zzz,800\ nm}>$ over all measurements. The only exception is compound [**10**]I, for which a small slope is observed that appears to be slightly above statistical uncertainty. However, the intercept and the average are still in statistical agreement. A general conclusion is that for the HRS measurements at 800 nm, possible multiphoton contributions did not enhance the first hyperpolarizability values above statistical uncertainty.

Acknowledgements

S.S. is indebted to Prof. Y. Geerts for the opportunity to conduct an independent research program in his laboratory and for generous financial support. This research is in part supported by the University of Leuven (GOA/2006/03). We thank Prof. M. Zeller (Youngstown State University, Ohio, USA) for the collection of the XRD dataset of [**3a**]I, R. de Borger and Prof. C. Van Alsenoy (University of Antwerpen) for computer time and assistance, and M. Antal (ULB) for the technical assistance. I.A. is a postdoctoral researcher of FWO-V.

References

[1] Chemla DS, Zyss J, editors. Nonlinear optical properties of organic molecules and crystals, vols. 1 and 2. Orlando, USA: Academic Press; 1987.
[2] Papadopoulos MG, Sadlej AJ, Leszczynski J, editors. Non-linear optical properties of matter: from molecules to condensed phases. Dordrecht, The Netherlands: Springer; 2006.
[3] Marder SR, Perry JW, Schaefer WP. Science 1989;245(4918):626–8.
[4] Coe BJ, Harris JA, Asselberghs I, Wostyn K, Clays K, Persoons A, et al. Adv Funct Mater 2003;13(5):347–57.
[5] Coe BJ, Harris JA, Brunschwig BS, Garin J, Orduna J. J Am Chem Soc 2005;127(10):3284–5.
[6] Coe BJ, Harris JA, Hall JJ, Brunschwig BS, Hung S-T, Libaers W, et al. Chem Mater 2006;18(25):5907–18.
[7] Zheng J, Huang C-H, Huang Y-Y, Wu D-G, Wei T-X, Yu A-C, et al. New J Chem 2000;24(5):317–21.
[8] Dirk CW, Katz HE, Schilling ML, King LA. Chem Mater 1990;2(6):700–5.
[9] Jen AKY, Rao VP, Wong KY, Drost KJ. J Chem Soc Chem Commun 1993;1:90–2.
[10] Abbotto A, Bradamante S, Facchetti A, Pagani GA. J Org Chem 1997;62(17):5755–65.
[11] Wang Y-K, Shu C-F, Breitung EM, McMahon RJ. J Mater Chem 1999;9(7):1449–52.
[12] Raposo MMM, Sousa AMRC, Kirsch G, Cardoso P, Belsley M, Matos De, et al. Org Lett 2006;8(17):3681–4.
[13] Facchetti A, Beverina L, van der Boom ME, Dutta P, Evmenenko G, Shukla AD, et al. J Am Chem Soc 2006;128(6):2142–53.
[14] Raposo MMM, Sousa AMRC, Fonseca AMC, Kirsch G. Tetrahedron 2006;62(15):3493–501.
[15] Batista RMF, Costa SPG, Malheiro EL, Belsley M, Raposo MMM. Tetrahedron 2007;63(20):4258–65.
[16] Razus AC, Birzan L, Surugiu NM, Corbu AC, Chiraleu F. Dyes Pigments 2007;74(1):26–33.
[17] Batista RMF, Costa SPG, Belsley M, Raposo MMM. Tetrahedron 2007;63(39):9842–9.
[18] Guo K, Hao J, Zhang T, Zu F, Zhai J, Qiu L, et al. Dyes Pigments 2008;77(3):657–64.
[19] Albert IDL, Marks TJ, Ratner MA. J Am Chem Soc 1997;119(28):6575–82.
[20] Ma X, Liang R, Yang F, Zhao Z, Zhang A, Song N, et al. J Mater Chem 2008;18(15):1756–64.
[21] Chou S-SP, Sun D-J, Huang J-Y, Yang P-K, Lin H-C. Tetrahedron Lett 1996;37(40):7279–82.
[22] Meier H. Angew Chem Int Ed 2005;44(17):2482–506.
[23] Wuerthner F, Effenberger F, Wortmann R, Kraemer P. Chem Phys 1993;173(2):305–14.
[24] Bedworth PV, Cai Y, Jen A, Marder SR. J Org Chem 1996;61(6):2242–6.
[25] Mignani G, Leising F, Meyrueix R, Samson H. Tetrahedron Lett 1990;31(33):4743–6.
[26] Costa SPG, Batista RMF, Cardoso P, Belsley M, Raposo MMM. Eur J Org Chem 2006;17:3938–46.
[27] Kabatc J, Jedrzejewska B, Orlinski P, Paczkowski J. Spectrochim Acta Part A 2005;62(1–3):115–25.
[28] Gromov SP, Sergeev SA, Druzhinin SI, Rusalov MV, Uzhinov BM, Kuz'mina LG, et al. Russ Chem Bull 1999;48(3):525–36.

[29] Lemaur V, Cornil J, Didier D, Mujawase A, Sergeyev S. Helv Chim Acta 2007;90:2087–95.
[30] Hotta S, Goto M, Azumi R, Inoue M, Ichikawa M, Taniguchi Y. Chem Mater 2004;16(2):237–41.
[31] (a) Kobatake S, Kuma S, Irie M. Bull Chem Soc Jpn 2004;77(5):945–51; (b) Kühni J, Belser P. Org Lett 2007;9(10):1915–8.
[32] Reichardt C. Chem Rev 1994;94:2319–58.
[33] Blanchard-Desce M, Alain V, Bedworth P, Marder SR, Fort A, Runser C, et al. Chem Eur J 1997;3:1091–104.
[34] Lawrentz U, Grahn W, Lukaszuk K, Klein C, Wortmann R, Feldner A, et al. Chem Eur J 2002;8:1573–90.
[35] Marder SR, Gorman CB, Meyers F, Perry JW, Bourhill G, Brédas J-L, et al. Science 1994;265:632–5.
[36] Meier H, Stalmach U, Kolshorn H. Acta Polym 1997;48(9):379–84.
[37] Meier H, Gerold J, Jacob D. Tetrahedron Lett 2003;44(9):1915–8.
[38] Coe BJ, Jones LA, Harris JA, Brunschwig BS, Asselberghs I, Clays K, et al. J Am Chem Soc 2004;126(12):3880–91.
[39] Gonzalez M, Segura JL, Seoane C, Martin N, Garin J, Orduna J, et al. J Org Chem 2001;66(26):8872–82.
[40] Meier H, Muehling B, Gerold J, Jacob D, Oehlhof A. Eur J Org Chem 2007;4:625–31.
[41] Meier H, Petermann R, Gerold J. Chem Commun 1999;11:977–8.
[42] Bures F, Schweizer WB, May J, Boudon C, Gisselbrecht J-P, Gross M, et al. Chem Eur J 2007;13(19):5378–87.
[43] Frisch MJ, Trucks GW, Schlegel HB, Scuseria GE, Robb MA, Cheeseman JR, et al. Gaussian 03, Revision C.02, Gaussian, Inc., Wallingford CT, 2004.
[44] Sheldrick GM. Acta Crystallogr Sect A Found Crystallogr 2008;A64(1):112–22.
[45] Olbrechts G, Strobbe R, Clays K, Persoons A. Rev Sci Instrum 1998;69(6):2233–41.
[46] Clays K, Persoons A. Phys Rev Lett 1991;66(23):2980–3.